International Journal of Cardiology 280 (2019) 142–151

Contents lists available at ScienceDirect

International Journal of Cardiology

journal homepage: www.elsevier.com/locate/ijcard

Silencing salusin β ameliorates heart failure in aged spontaneously hypertensive rats by ROS-relative MAPK/NF-κB pathways in the paraventricular nucleus

Hong-Bao Li [a], Xiao-Jing Yu [a], Juan Bai [a], Qing Su [a], Mo-Lin Wang [a,b], Chan-Juan Huo [a], Wen-Jie Xia [a], Qiu-Yue Yi [c], Kai-Li Liu [a], Li-Yan Fu [a], Guo-Qing Zhu [d], Jie Qi [a,*], Yu-Ming Kang [a,*]

[a] Department of Physiology and Pathophysiology, Xi'an Jiaotong University School of Basic Medical Sciences, Key Laboratory of Environment and Genes Related to Diseases of Ministry of Education, Xi'an Jiaotong University, Xi'an 710061, China
[b] Department of immunology, School of Basic Medical Sciences, Jiamusi University, Jiamusi 154007, China
[c] Department of Cardiovascular Surgery, First Affiliated Hospital of Xi'an Jiaotong University, Xi'an 710061, China
[d] Key Laboratory of Cardiovascular Disease and Molecular Intervention, Department of Physiology, Nanjing Medical University, Nanjing 210029, China

ARTICLE INFO

Article history:
Received 25 September 2018
Received in revised form 25 November 2018
Accepted 4 December 2018
Available online 7 December 2018

Keywords:
Paraventricular nucleus
Heart failure
Salusin β
NF-κB
Reactive oxygen species

ABSTRACT

Objective: Sustained hypertension is a major cause of heart failure in aging hypertensive patients. Salusin β, a novel bioactive peptide of 20 amino acids, has been reported to participate in various cardiovascular diseases, including hypertension. We therefore hypothesized that central knockdown of salusin β might be effective for hypertension-induced heart failure treatment.

Methods and results: Eighteen-month-old male aged spontaneously hypertensive rats (SHR) with heart failure and WKY rats were microinjected with either a specific adenoviral vector encoding salusin β shRNA (Ad-Sal-shRNA) or a scramble shRNA (Ad-Scr-shRNA) in the hypothalamic paraventricular nucleus (PVN) for 4 weeks. Radiotelemetry and echocardiography were used for measuring blood pressure and cardiac function, respectively. Blood samples and heart were harvested for evaluating plasma norepinephrine, tyrosine hydroxylase, and cardiac morphology, respectively. The mesenteric arteries were separated for measurement of vascular responses. The PVN was analyzed for salusin β, proinflammatory cytokines (PICs), mitogen-activated protein kinase (MAPK), NF-κB, and reactive oxygen species (ROS) levels. Compared with normotensive rats, aging SHR with heart failure had dramatically increased salusin β expression. Silencing salusin β with Ad-Sal-shRNA attenuated arterial pressure and improved autonomic function, cardiac and vascular dysfunction in aging SHR with heart failure, but not in aging WKY rats. Knockdown of salusin β significantly reduced paraventricular nucleus PICs levels, MAPK and NF-κB activity, and ROS levels in aging SHR with heart failure.

Conclusion: These data demonstrate that in aging SHR, the heart failure that was developed during the end stage of hypertension could be ameliorated by silencing salusin β.

1. Introduction

Most elderly hypertensive patients display impaired autonomic function, elevated blood pressure (BP), and cardiac and vascular dysfunction. Importantly, long term blood pressure overload [1], impaired autonomic function [2,3], stable cardiac hypertrophy and vascular senescence-related abnormalities [3,4] may lead to heart failure. Therefore, reducing the BP, improving autonomic function, and controlling heart and vasculature remodeling process by drugs are clearly vital issues for treatment of hypertension-induced heart failure.

Salusin β was initially translated from a torsion dystonia-related gene mRNA [5]. A previous study indicated that rat salusin β has high homology with human salusin β [6]. Salusin β immunopositive cells have been widely found in central and peripheral tissues [7,8]. It has

Abbreviations: SHR, spontaneously hypertensive rats; WKY, Wistar–Kyoto rats; Ad-Sal-shRNA, adenoviral vectors encoding salusin β shRNA; Ad-Scr-shRNA, scramble shRNA; PVN, hypothalamic paraventricular nucleus; PICs, proinflammatory cytokines; MAPK, mitogen-activated protein kinase; ROS, reactive oxygen species; NF-κB, nuclear factor kappa-B; BP, blood pressure; HR, heart rate; SBP, systolic blood pressure; PI, pulse interval; sBRG, spontaneous cardiac baroreflex gain; LVEDP, left ventricular end-diastolic pressure; LVSP, left ventricular systolic pressure; LVEF, left ventricular ejection fraction; LVFS, left ventricular fractional shorting; T-AOC, total antioxidant capacities; SOD, superoxide dismutase; GSH, glutathione; GSSG, oxidized glutathione; MDA, lipid peroxidation malonaldehyde.

* Corresponding authors at: Department of Physiology & Pathophysiology, School of Basic Medical Sciences, Xi'an Jiaotong University Health Science Center, Xi'an 710061, China.
E-mail addresses: jie-qi@xjtu.edu.cn (J. Qi), ykang@mail.xjtu.edu.cn (Y.-M. Kang).

https://doi.org/10.1016/j.ijcard.2018.12.020
0167-5273/

been found that central salusin β is involved in sympathetic activation and hypertension associated with arginine vasopressin release [9], and inhibition of endogenous salusin β contributes to attenuate sympathoexcitation and hypertension [10]. Salusin β has been indicated to promote the formation of human macrophage foam cells and monocyte adhesion by ROS production in atherosclerosis [11,12]. Inhibition of salusin β in human vascular smooth muscle cells reduces ROS production [11]. Salusin β has been also reported to participate in the inflammatory processes associated with atherosclerosis, hypertension, and myocardial ischemic disease [13].

However, there is little information examining the effect of central knockdown of salusin β in clinically relevant elderly hypertensive animal models. The aged spontaneously hypertensive rats (SHR) is a model utilized for understanding mechanism of hypertension-induced heart failure and effective strategies for its treatment. The aged hypertension model provides many similarities to elderly hypertensive patients in pathophysiological development, neuroendocrine changes, clinical courses and secondary diseases [14,15]. Thus, aged SHR was used as a hypertension-induced heart failure animal model in the present study. Therefore, we designed this study to observe the roles and the downstream mechanism of silencing salusin β in the hypothalamic paraventricular nucleus in aging spontaneously hypertensive rats with heart failure.

2. Methods

2.1. Animals

Eighteen-month-old aging male SHR and WKY rats were obtained from the Charles River Laboratory and housed in individual standard cages in a climate-controlled room on a 12:12-h light-dark cycle with standard rat chow and tap water ad libitum. This study involved procedures that received approval from the Experimental Animal Care and Use Committee of Xi'an Jiaotong University and were performed in accordance with the Guide for Care and Use of Laboratory Animals published by the US National Institutes of Health (NIH publication, 8th edition, 2011).

2.2. Arterial blood pressure measurements and power spectral analysis

Arterial blood pressure in aging SHR and WKY rats was measured by a telemetry system (Data Sciences International, MN, USA) as described previously [3,16,17]. Briefly, animals were anesthetized using a 2% isoflurane-oxygen mixture. After the abdominal wall was exposed via a midline incision, the abdominal aorta was separated, and the catheter of the transmitter was inserted into the abdominal aorta. After the transmitter implantation, rats were injected with buprenorphine (0.1 mg/kg) for pain control and allowed to recover for one week. The BP and heart rate (HR) data were measured and recorded from the conscious rats using a computer with software (DATAQUEST, MN, USA) during the dark and light periods for 5 weeks. The HR was derived from the pulse interval (PI). Baseline BP and HR were recorded for one week before the viral transfer to PVN. Spectral analysis of systolic blood pressure (SBP) was performed using Hey Presto software as previously described [18,19]. The frequency in this study was defined as follow: low frequency (LF, 0.27–0.75 Hz) and high frequency (HF, 0.75–3.3 Hz). The ratio of LF/HF (reflective of vasovagal balance) was calculated. Spontaneous changes in SBP and pulse interval (PI) were performed in order to obtain the spontaneous cardiac baroreflex gain (sBRG) as described previously [3,17].

2.3. Preparation and construction of adenovirus salusin β shRNA

The construction and preparation of the adenoviral vector containing shRNA were performed by Genomeditech (Shanghai Genomeditech Biotechnology, Shanghai, China), as described previously [12,20]. In this study, the adenovirus-mediated shRNA vector targeting salusin β was subjected to downregulation of salusin β in the PVN. The rat salusin β-specific shRNA sequences (Sense: 5'-gatccGCCCTTCTTGGGTTGTGTATGTTCAA GAGACATACACAACCCAAGAAGGGCTTTTTTa-3′ and Antisense: 5'-agcttAAAAAAGCCCT TCTTGGGTTGTGTATGTCTCTTGAACATACACAACCCAAGAAGGGCg-3′) were cloned into an adenoviral vector to construct Ad-Sal-shRNA. The viral vector contained a green fluorescent protein (GFP) reporter gene. The scrambled shRNA sequences (Sense: 5'-gatccGTTC TCCGAACGTGTCACGTTTCAAGAGAACGTGACACGTTCGGAGAACTTTTTTACGCGTg-3′ and Antisense: 5'-aattcACGCGTAAAAAAGTTCTCCGAACGTGTCACGTTCTCTTGAAACGTGACACG TTCGGAGAACg-3′) were used for the control shRNA, as described previously [20].

2.4. Adenovirus microinjection into the hypothalamic paraventricular nucleus

Rats were allowed to recover for 1 week following the experimental protocol, after which time a continuous baseline recording of BP and HR was made for an additional week. These rats were then anesthetized using a 2% isoflurane-oxygen mixture and placed in a stereotaxic instrument. The coordinates for the PVN were 1.8 mm posterior to the bregma, 0.4 mm from midline, and 7.9 mm ventral to dura according to the standard atlas of rats [21,22]. Then the skull was exposed through an incision on the midline of the scalp, and a stainless steel double cannula (Plastics One, Inc) was implanted into the PVN. The dental acrylic and 2 stainless steel screws were used for fixing the cannula to the cranium. The either aging SHR or WKY rats were randomly divided into four groups ($n = 14$ for each group), which were respectively subjected to injection of adenovirus expressing scrambled shRNA (Ad-Scr-shRNA) or adenovirus expressing salusin β shRNA (Ad-Sal-shRNA, 2×10^{10} plaque forming units/ml, 1 μl) using a 32-gauge Hamilton syringe (1 μl). The detailed experimental protocol is shown in Fig. S1.

2.5. Measurement of cardiac function in rats

A Vivid7 ultrasound machine (GE Healthcare, Waukesha, WI) was used for echocardiographic measurements as previously described [23]. Briefly, rats were anesthetized using a 2% isoflurane-oxygen mixture. Two-dimensional M-mode echocardiography was performed in the short-axis of the left ventricular (LV) at the level of the papillary muscles. The echocardiography parameters included LV internal dimensions, interventricular septum thickness, LV posterior wall dimensions, LV ejection fraction (LVEF) and LV fractional shorting (LVFS).

2.6. Measurement of haemodynamic parameters

Rats were anesthetized with the 2% isoflurane-oxygen mixture. The right carotid artery was cannulated with a micromanometer tipped catheter for BP, LV end-diastolic pressure (LVEDP) and left ventricular systolic pressure (LVSP) measurements. The BP, LVEDP and LVSP were monitored with a pressure transducer. Chart 7 software was used for recording and calculating BP and heart rate (HR). LVEDP and LVSP were directly derived from LV pressure waveforms. Parameters of diastolic and systolic function, maximal rate of pressure development (dp/dt_{max}) and maximal rate of pressure decline (dp/dt_{min}) were calculated by the software program.

2.7. Blood and tissue sample collection

Rats were euthanized using a 2% isoflurane-oxygen mixture and blood samples were collected from the abdominal aorta, quickly separated and stored at −80 °C until use. The brain and heart were quickly collected, and the left ventricles (LV) were separated and weighed. The LV weight/body weight (BW) was calculated as an indicator of heart function. The mesenteric arteries were separated and cut into cylindrical segments (1–2 mm in length) for the vessel ring experiments.

2.8. Tissue microdissection

The hypothalamic tissue including the PVN was dissected from freshly frozen brains as previous described [24]. In brief, a coronal section was cut from −0.90 to −2.15 mm posterior to the bregma according to Paxinos and Watson sterotaxic coordinates. These sections were mounted on slides, and both sides of the PVN tissues were isolated from each brain using a brain punch-out technique. The PVN tissue was stored at −80 °C until analyzed for real-time RT-PCR or Western blotting.

2.9. Vessel ring myograph experiments

The isometric tension of isolated arteries were recorded by sensitive myograph system (Dual Wire Myograph System 610A) as described previously [25]. The vessel segments were immersed in a modified Tyrode buffer solution and aerated with a 5% CO_2 in 95% O_2 gas mixture. L-phenylephrine (10^{-7} mol/l) was used to determine the contractile function of vessel rings. Increasing concentrations of acetylcholine (10^{-9} to 10^{-4} mol/l) or sodium nitroprusside (10^{-9} to 10^{-4} mol/l) were administered to obtain cumulative concentration-response curves of vascular segment. The rings were incubated with *N*-acetyl-L-cysteine (NAC, 10 μM), a ROS scavenger, for 30 min, and endothelium-dependent responses were then measured. A computer with a PowerLab Unit (ADInstruments, Oxford, UK) was used for data measurement and analysis.

2.10. Immunohistochemistry

Immunohistochemistry labeling for detecting the expression of salusin β (1:400, Bachem, Bubendorf, Switzerland), Fra-like (Fra-LI, a marker of chronic neuronal activation; 1:100, Abcam Inc), and tyrosine hydroxylase (TH; 1:500, Abcam Inc., USA) in the PVN was performed as we previously reported [26,27]. The expression of salusin β positive staining cells in the PVN was measured by averaging the numbers of five sections for each rat. TH-, and Fra-like-positive neurons within a window superimposed over the subregions of the PVN were counted and the data were reported as an average value for each subregion.

2.11. Immunofluorescent double-labeled staining

The procedure for immunofluorescent staining was described previously [27,28]. Briefly, rats were euthanized and then perfused with 200 ml of PBS followed by 400 ml of paraformaldehyde. Rat brains were collected in a 4% paraformaldehyde solution, and then transferred to 30% sucrose for 48 h. Brain tissue was rapidly frozen and cut in a

cryostat. 18-μm-thick sections were blocked for 30 min in 2% goat serum in PBS containing 0.3% Triton X100. Then, the brain sections were incubated with rabbit anti-human salusin β antibody (1:400, Bachem, Bubendorf, Switzerland), mouse anti-neuronal nuclei (NeuN) antibody (1:300; Abcam Inc., USA), or mouse anti-glial fibrillary acid protein (GFAP) (1:100; Abcam Inc., USA). Corresponding secondary antibodies were used in order to detect the primary antibody, which included CY3-labeled anti- rabbit antibody (at 1:200; green fluorescence; Chemicon International, Temecula, California, USA) and fluorescein isothiocyanate (FITC)-labeled anti-mouse antibody (at 1:200 dilution; red fluorescence; Cell Signaling Technology, MA, USA). The immunofluorescent double-labeled staining was detected using a confocal laser-scanning microscope.

2.12. Total RNA isolation and quantitative real-time RT-PCR

The mRNA levels of monocyte chemotactic protein (MCP-1), tumor necrosis factor-alpha (TNF-α), IL-1β, IL-6, and NAD(P)H oxidase subunit 2 and 4 (NOX2 and NOX4) in the PVN tissues ($n = 6$/group) were determined by real-time RT-PCR using specific primers (Supplemental Table 1). A standard procedure for total RNA extraction and real-time RT-PCR was performed as previously described [10,26]. Briefly, total RNA was prepared using Trizol reagent. The mRNA concentration in the samples was measured and a total of 1 μg RNA was reversely transcribed with a high-capacity cDNA reverse transcription kit (Bio-Rad, USA). Quantitative real-time PCR with iTaq SYBR™ Green Supermix with ROX was used for cDNA amplification with gene-specific primers. Data were processed by the $2^{-\Delta\Delta CT}$ method, and normalized by the expression of β-actin.

2.13. Western blot

The protein levels of salusin β, MCP-1, TNF-α, IL-1β, IL-6, NOX2, NOX4, 4-HNE, p65 subunit of NF-κB, p-p38, total p38, p-ERK1/2, total ERK1/2, p-JNK and total JNK in the PVN were measured and analyzed by Western blot. The standard protocol and procedure of Western blot were performed, as described previously [27,29]. Briefly, the rat brains were quickly removed and stored at −80 °C before the experiment. After the measurement of protein concentration using a Bradford assay, the protein was loaded onto a 10% or 12% SDS-PAGE gel and then transferred to a polyvinylidene fluoride membrane. The membranes were then subjected to immunoblot analysis with the primary antibodies. Specific antibodies used included the following: MCP-1, TNF-α, IL-1β, IL-6, at 1:1000 dilution; salusin β, at 1:800 dilution; NOX2, NOX4, 4-HNE, p65 subunit of NF-κB, at 1:2000 dilution; p-p38, p-ERK1/2, p-JNK, at 1:3000 dilution; and total p38, total ERK1/2, total JNK, at 1:2000 dilution; The following antibodies were commercially obtained: MCP-1, TNF-α, IL-1β, IL-6 and p65 subunit of NF-κB (Santa Cruz Biotechnology, Santa Cruz, CA); salusin β (Bachem, Bubendorf, Switzerland); p-p38, p-ERK1/2, and p-JNK (Cell Signaling Technology, Danvers, MA); and NOX2, NOX4, 4-HNE, total p38, total ERK1/2 and total JNK (Abcam Inc., MA, USA). After the blots were washed with TBST three times for 10 min each time, they were incubated with horseradish peroxidase labeled secondary antibody (at 1:6000 dilution, Santa Cruz Biotechnology) for 1 h at 37 °C. The Image Lab analysis software (Bio-Rad, CA, USA) was used for quantifying the density of the bands. The level of target proteins was normalized to β-actin (Thermo Scientific, USA).

2.14. Measurement of salusin β, norepinephrine (NE) and TH

Salusin β, NE and TH were measured ($n = 6$/group) using a norepinephrine ELISA kit (Abnova, Taiwan), a salusin β ELISA kit (Uscn Life Science, Houston, TX, USA) and a TH ELISA kit (Uscn Life Science, Houston, TX, USA), respectively, per the manufacturer's guidelines.

2.15. Assessment of antioxidant status

The total antioxidant capacities (T-AOC), lipid peroxidation malonaldehyde (MDA), superoxide dismutase (SOD), glutathione (GSH) and oxidized glutathione (GSSG) in the PVN were measured using commercial ELISA kits (Nanjing Jiancheng, Nanjing, China) and quantified according to the manufacturer's guidelines.

2.16. Fluorescent-labeled dihydroethidium (DHE) fluorescence staining

Superoxide production in the PVN, heart and mesenteric artery was determined using DHE (Invitrogen, Molecular Probes, Carlsbad, CA) staining as previously described [3,10,30]. In brief, rat brain, heart and mesenteric artery were taken out from −80 °C refrigerator, and immediately embedded in OCT compound. Frozen sections were cut from the tissues containing the PVN, heart and mesenteric artery, and incubated in DHE (15 mM) for 30 min at 4 °C and protected from light. After being washed with PBS three times for 10 min each time, these sections were observed using a fluorescence microscope. Fluorescence intensity was analyzed and quantified with NIH ImageJ software.

2.17. Statistical analysis

All data are expressed as means ± SE and analyzed using either two-way ANOVA or one-way ANOVA with a post hoc Bonferroni posttest. Differences were considered significant if a probability value of $P < 0.05$ was achieved. Graph Pad Prism software was used for the analysis and graph generation.

3. Results

3.1. Salusin β expression

First, we compared the positive neurons of salusin β in the PVN in aging SHR and WKY rats using immunohistochemistry and observed a significant increase in salusin β expression within the PVN of aging SHR (Fig. S2A, 2B and 2C). ELISA results also revealed that the concentration of salusin β in the PVN of the aging SHR was higher than that in aging WKY rats (Fig. S2D). Next, we observed the cell-type distribution of salusin β in the PVN using a double-labeling immunofluorescence technique. The majority of salusin β was co-localized with a neuronal marker NeuN; whereas, almost none of salusin β-positive cells were co-localized with the astrocyte marker GFAP in the PVN of aging SHR (Fig. S2E). Finally, we observed that the concentration of salusin β significantly increased in the myocardium (Fig. S3A) and mesenteric artery (Fig. S3B) of aging SHR as compared with aging WKY rats, respectively. Ad-Sal-shRNA reduced the salusin-β contents of myocardium and mesenteric artery in aging SHR (Fig. S3).

3.2. Localization and the effects of the adenoviral delivery of salusin β expression in the PVN

Two weeks after bilateral intra-PVN infusion of Ad-Sal-shRNA, highly robust GFP (green fluorescent protein) expression was detected in the PVN but not in the subfornical organ or the supraoptic nucleus (Fig. S4A), indicating that the Ad-shRNA that was infused into the PVN did not leak into the cerebral ventricles. There was no GFP expression in the brain sections from rats without adenovirus infusion (Fig. S4A). To observe the effective of salusin β knockdown, we performed Western blot analyses and ELISA studies for the determination of the level of salusin β in the PVN. We found that salusin β protein level (Fig. S4B) and concentration (Fig. S4C) were reduced in aging SHR treated with Ad-Sal-shRNA compared with that in the aging SHR treated with Ad-Scr-shRNA (the control vector shRNA-GFP).

3.3. Effect of salusin β knockdown on systolic BP, HR and autonomic balance in aging SHR and WKY rats

The SBP and HR in the aging SHR were significantly increased when compared to that in the aging WKY rats. Two weeks after intra-PVN infusion of Ad-Sal-shRNA, there was no significant difference in SBP and HR in the aging WKY rats, and caused significant decreases in SBP and HR in aging SHR (Fig. 1A and B). To confirm the effect of Ad-Sal-shRNA, mean arterial pressure (MAP) and HR were measured during the acute experiment in anesthetized state. MAP in anesthetized state was significantly increased in aging SHR when compared with those in aging WKY, which were prevented by intra-PVN salusin β knockdown (Supplemental Table 2).

Cardiac spontaneous baroreflex gain [sBRG(PI)] and high frequency (HF) band of the pulse interval (PI) (reflective of cardiac parasympathetic tone) were attenuated in the aging SHR compared to that in the aging WKY rats. Bilateral intra-PVN infusion of Ad-Sal-shRNA was able to increase sBRG(PI) and HF(PI) in aging SHR (Fig. 1C and E). In addition, the low frequency (LF) band of SBP (reflective of vasomotor sympathetic activity) and LF/HF (reflective of vasovagal balance) were increased in the aging SHR compared with that in the aging WKY, which were normalized by intra-PVN salusin β knockdown (Fig. 1D and F). No significant changes were observed in aging WKY rats treated with Ad-Sal-shRNA (Fig. 1C-F).

3.4. Effect of salusin β knockdown on cardiac morphology in aging SHR and WKY rats

At the end of the experiment, there were no significant differences in body weight among the four groups (Supplemental Table 2). However,

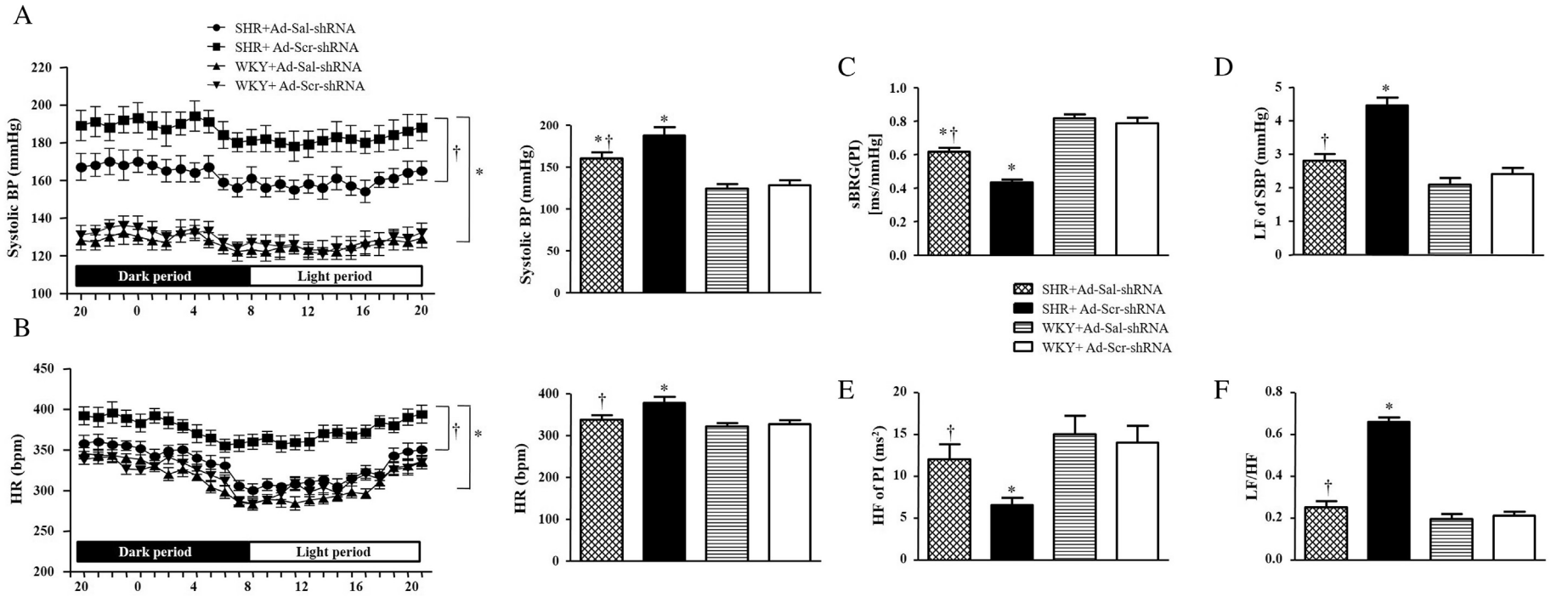

Fig. 1. Effects of bilateral intra-PVN infusion of Ad-Sal-shRNA on systolic BP, HR and autonomic function in aging SHR and WKY rats. In (A), the left panel shows hourly recordings of systolic BP over 24 h using telemetry, and the right panel indicates 24-h-averaged systolic BP. In (B), the left panel shows hourly recordings of HR over 24 h using telemetry, and the right panel indicates 24-h-averaged HR. (C) sBRG(PI): cardiac spontaneous baroreflex gain. (D) LF(SBP): vasomotor sympathetic tone. (E) HF(PI): cardiac parasympathetic drive. (F) LF/HF: vasovagal balance. sBRG: spontaneous baroreflex gain, LF: low frequency, HF: high frequency. $n = 7$ rats/group. Values are represented as the means ± SE. *$P < 0.05$ versus WKY groups (WKY + Ad-Scr-shRNA or SHR + Ad-Sal-shRNA); †$P < 0.05$ SHR + Ad-Sal-shRNA versus SHR + Ad-Scr-shRNA.

LVW/BW and LVW/Tibia values were significantly increased in the SHR + Ad-Scr-shRNA group compared with that in the WKY group. A significant decrease in LVW/BW and LVW/Tibia were observed in the Ad-Sal-shRNA treatment group compared with that in the SHR + Ad-Scr-shRNA group (Supplemental Table 2).

3.5. Effect of salusin β knockdown on cardiac function and remodeling in aging SHR and WKY rats

In comparison to untreated aging WKY rats with the same age, the LV systolic pressure (LVSP) and LV end-diastolic pressure (LVEDP) of aging SHR were significantly increased. Ad-Sal-shRNA treatment could significantly decrease LVSP and LVEDP in aging SHR, but not in aging WKY rats (Supplemental Table 2). As shown in supplemental Table 2, the dp/dt_{max} (maximal rate of pressure development) and dp/dt_{min} (maximal rate of pressure decline) were also reduced in aging SHR compared with aging WKY rats, which were increased by Ad-Sal-shRNA treatment.

Echocardiography revealed that LV internal dimensions in systole (LVIDs) and LV internal dimensions in diastole (LVIDd) were increased in aging SHR compared to that in the aging WKY rats, which were attenuated by Ad-Sal-shRNA (Supplemental Table 3). As shown in supplemental Table 3, the LV ejection fraction (LVEF) and LV fractional shortening (LVFS)

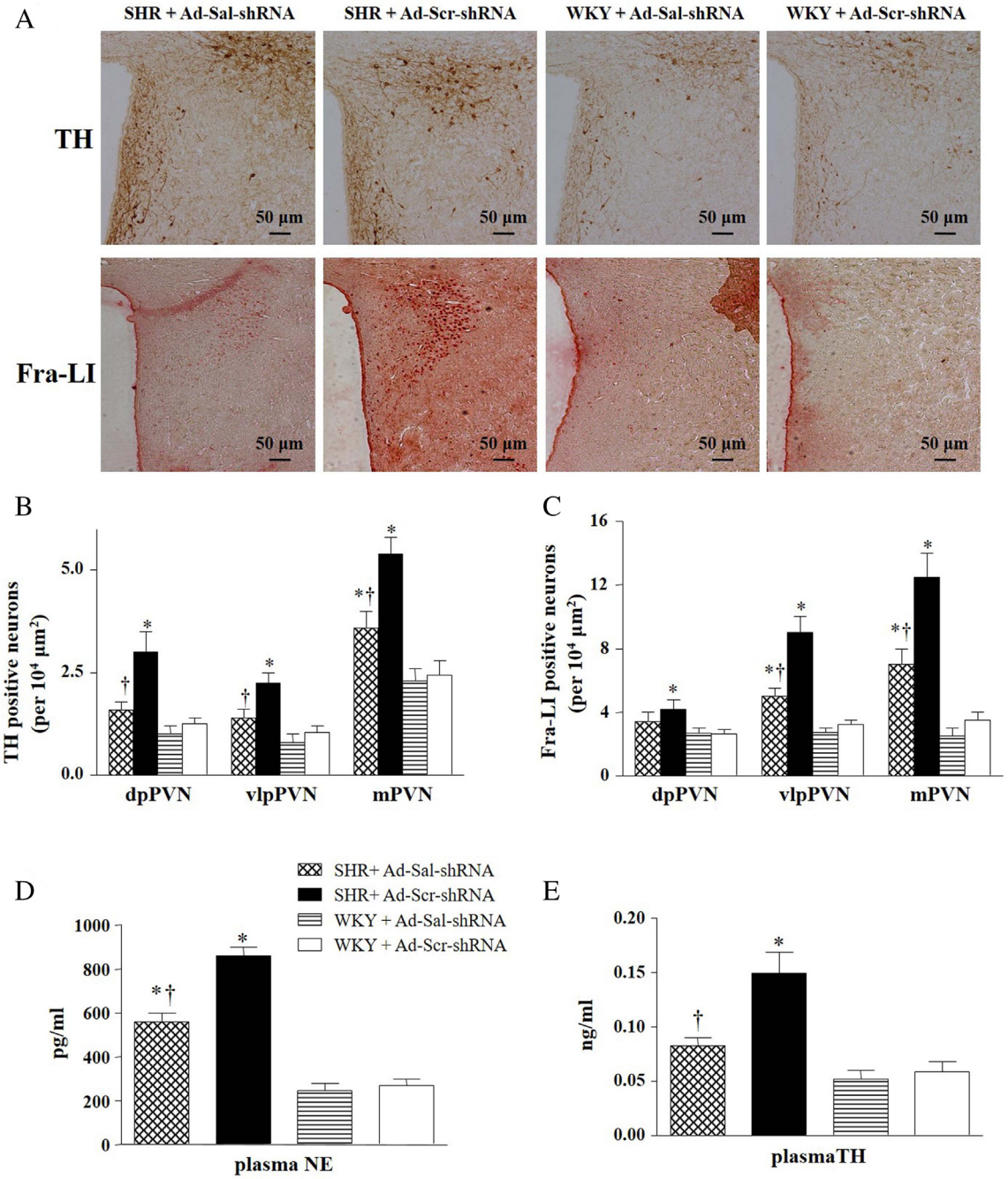

Fig. 2. Effects of bilateral intra-PVN infusion of Ad-Sal-shRNA on neuronal activity and sympathetic excitation in aging SHR and WKY rats. (A) Immunohistochemistry for detecting Fra-like (a marker of chronic neuronal activation) and tyrosine hydroxylas (TH, an indirect index of sympathetic activity) positive neurons in the PVN. (B, C) Bar graph showing the average number of neurons with TH- and Fra-like-positive neurons within a window superimposed over the dorsal parvocellular (dpPVN), ventrolateral parvocellular (vlpPVN), and magnocellular (mPVN) subregions of the PVN. (D) Plasma norepinephrine (NE) levels. (E) Plasma tyrosine hydroxylas levels. 3 V, third ventricle. n = 7 rats/group. Values are represented as the means ± SE. *$P < 0.05$ versus WKY groups (WKY + Ad-Scr-shRNA or SHR + Ad-Sal-shRNA); †$P < 0.05$ SHR + Ad-Sal-shRNA versus SHR + Ad-Scr-shRNA.

were significantly reduced in aging SHR than those in aging WKY rats, which were increased by Ad-Sal-shRNA treatment.

3.6. Effect of salusin β knockdown on vascular endothelial function in aging SHR and WKY rats

As indicated in Fig. S5A, vascular endothelium-dependent relaxation was significantly impaired in aging SHR compared to that in the aging WKY rats, which was ameliorated by Ad-Sal-shRNA. However, pretreatment with Nω-Nitro-L-arginine methyl ester hydrochloride almost completely abolished acetylcholine-induced vascular relaxation in all groups (Fig. S5B). There was no significant difference in sodium nitroprusside-induced endothelium independent vascular relaxation (Fig. S5C). To determine the influence of ROS on endothelial-dependent relaxation, the effects of NAC on acetylcholine-induced relaxation were assessed. In the arteries from SHR treated with Ad-Sal-shRNA rats, NAC improved the acetylcholine-induced relaxation as shown in Fig. S6.

3.7. Effect of salusin β knockdown on PVN neuronal activity and sympathetic excitation in aging SHR and WKY rats

Chronic neuronal excitation was reflected by Fra-like expression. As indicated in Fig. 2, the level of Fra-like in the PVN was upregulated in SHR + Ad-Scr-shRNA rats when compared to that in aging WKY rats. Interestingly, SHR treated with Ad-Sal-shRNA had significantly fewer Fra-LI-positive neurons in the subregions of PVN than SHR treated with Ad-Scr-shRNA. Norepinephrine (NE) and tyrosine hydroxylase (TH) are commonly used as indirect indicators of sympathetic activity in SHR. Plasma NE and TH levels were significantly lower in SHR treated with Ad-Sal-shRNA compared with that in the SHR treated with Ad-Scr-shRNA. Furthermore, the expression of TH-positive neurons in the subregions of PVN in SHR was also reduced by Ad-Sal-shRNA treatment (Fig. 2).

3.8. Effect of salusin β knockdown on PVN inflammation in aging SHR and WKY rats

As showed in Fig. 3, SHR + Ad-Scr-shRNA rats had higher levels of proinflammatory cytokines than in aging WKY rats. Treatment with Ad-Sal-shRNA for 4 weeks attenuated the expression of MCP-1, TNF-α, IL-1β and IL-6 in the PVN of aging SHR. No significant effect of salusin β knockdown on proinflammatory cytokines was observed in aging WKY rats (Fig. 3).

3.9. Effect of salusin β knockdown on NF-κB activity in aging SHR and WKY rats

As indicated in Fig. S7A, SHR + Ad-Scr-shRNA rats showed an increased p-IKKβ expression in the PVN when compared to that in

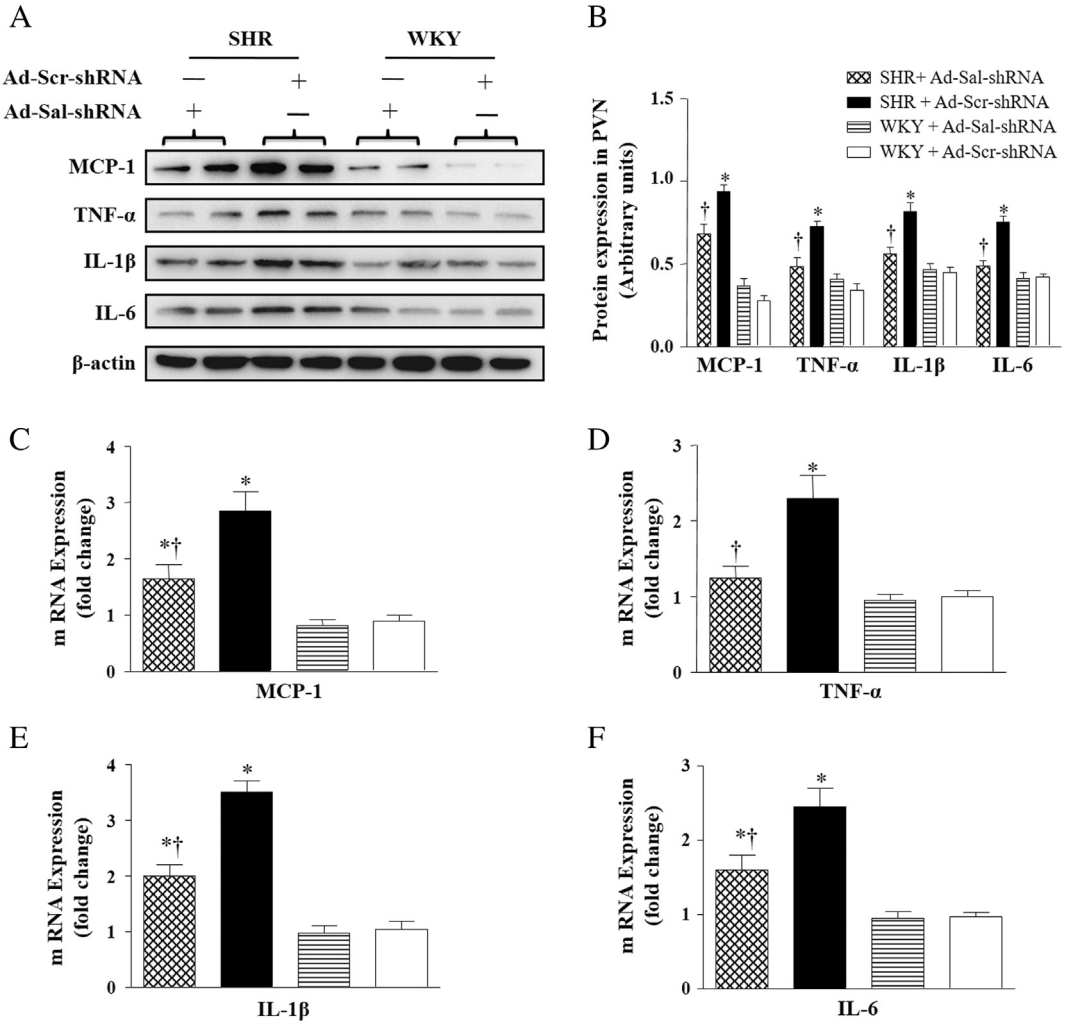

Fig. 3. Effects of bilateral intra-PVN infusion of Ad-Sal-shRNA on the levels of proinflammatory cytokines (PICs) within the PVN in aging SHR and WKY rats. (A) A representative immunoblot; and (B) densitometric analysis of protein expression of MCP-1, TNF-α, IL-1β and IL-6 in the PVN in aging SHR and WKY rats. (C—F) The mRNA expressions of MCP-1, TNF-α, IL-1β and IL-6 in the PVN in aging SHR and WKY rats. 3 V, third ventricle. n = 7 rats/group. Values are represented as the means ± SE. *$P < 0.05$ versus the WKY groups (WKY + Ad-Scr-shRNA or WKY + Ad-Sal-shRNA); †$P < 0.05$ SHR + Ad-Sal-shRNA versus SHR + Ad-Scr-shRNA.

aging WKY rats. SHR treated with Ad-Sal-shRNA had significantly fewer p-IKKβ-positive neurons expression in the PVN than that in SHR treated with Ad-Scr-shRNA. Western blot analysis revealed that the levels of increased p65 in nucleus and reduced p65 in cytoplasm in the PVN were ameliorated by Ad-Sal-shRNA treatment in aging SHR (Fig. S7B-E).

3.10. Effect of salusin β knockdown on MAPK signaling pathway in aging SHR and WKY rats

The MAPK is an important signal transduction molecule for inflammatory cytokines production. To determine whether the MAPK signaling pathway was participating in the effect of salusin β inhibition on inflammatory responses in the PVN, we identified the protein levels of p38 MAPK, ERK1/2, and JNK by western blotting. We observed that the phosphorylation of ERK1/2, p38MAPK and JNK in the PVN of SHR was significantly increased compared with their respective control groups (Fig. S8). However, salusin β knockdown with Ad-Sal-shRNA significantly attenuated the levels of p38MAPK, ERK1/2 and JNK in the PVN compared with SHR treated with Ad-Scr-shRNA (Fig. S8).

3.11. Effect of salusin β knockdown on NAD(P)H oxidase activity and reactive oxygen species in aging SHR and WKY rats

The subunits of NADPH oxidase NOX2 and NOX4 (major source of induced reactive oxygen species production) protein expression levels were higher in the PVN of aging SHR but not in aging WKY rats, which were normalized by Ad-Sal-shRNA treatment (Fig. 4A-D). Dihydroethidium (DHE) staining results further demonstrated that increased reactive oxygen species (ROS) generation was higher in the PVN of SHR, which was attenuated by Ad-Sal-shRNA (Fig. 4E).

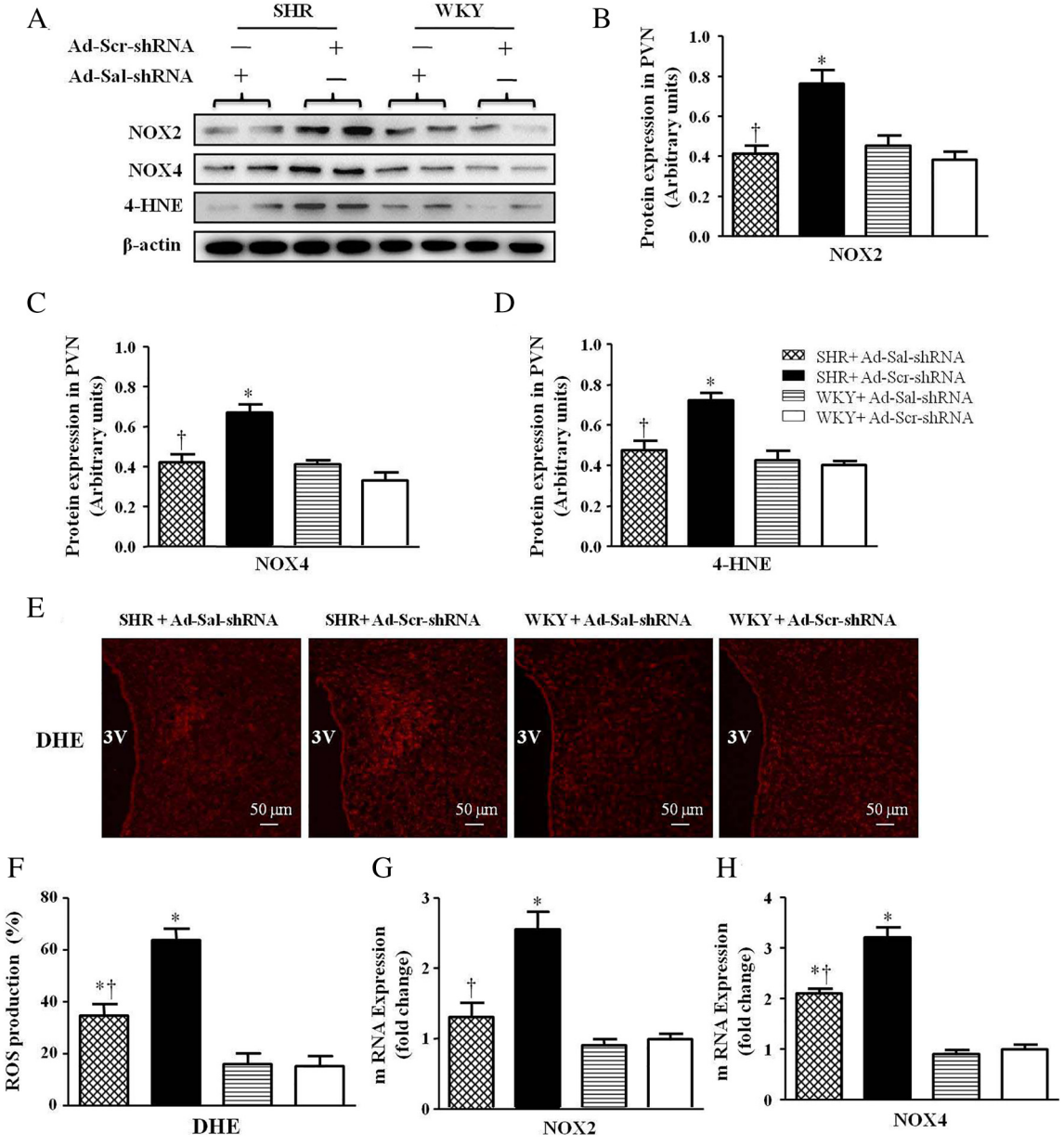

Fig. 4. Effects of bilateral intra-PVN infusion of Ad-Sal-shRNA on NAD(P)H oxidase activity and reactive oxygen species within the PVN in aging SHR and WKY rats. (A) A representative immunoblot; and (B, C and D) densitometric analysis of protein expression of NOX2, NOX4 and 4-HNE. (E) A representative immunofluorescence images from the PVN sections of each group showing superoxide production detected by dihydroethidium (DHE) staining (red fluorescence). (F) Bar graph showing the average fluorescence density of superoxide. (G, H) The mRNA expressions of NOX2 and NOX4 in the PVN in aging SHR and WKY rats. 3 V, third ventricle. n = 7 rats/group. Values are represented as the means ± SE. *$P < 0.05$ versus WKY groups (WKY + Ad-Scr-shRNA or WKY + Ad-Sal-shRNA); †$P < 0.05$ SHR + Ad-Sal-shRNA versus SHR + Ad-Scr-shRNA.

Real-time RT-PCR results also indicated that mRNA levels of NOX2 and NOX4 increased in aging SHR, which were reduced by salusin β knockdown (Fig. 4F-H). We also evaluated the levels of superoxide production in heart and vessel by DHE. Similarly, the levels of superoxide in heart and mesenteric artery were raised in SHR, which were normalized by salusin β knockdown (Fig. S9).

3.12. Effect of salusin β knockdown on antioxidant defense system in aging SHR and WKY rats

Various enzymatic and non-enzymatic antioxidant levels (the potential sources of ROS formation) in the PVN were measured by ELISA method. We observed that SHR + Ad-Scr-shRNA rats had lower levels of total antioxidant capacities (T-AOC), superoxide dismutase (SOD) and glutathione (GSH) compared with that in the aging WKY rats (Fig. S10). In addition, SHR + Ad-Scr-shRNA rats had higher levels of oxidized glutathione (GSSG) and lipid peroxidation malonaldehyde (MDA), and a reduced GSH/GSSG ratio in comparison to aging WKY rats (Fig. S10). Interestingly, SHR rats treated with Ad-Sal-shRNA had significantly increased T-AOC, SOD, and GSH activities, and upregulated the GSH/GSSG ratio, and decreased GSSG and MDA levels than SHR treated with Ad-Scr-shRNA (Fig. S10).

4. Discussion

Salusin β is an endogenous neuropeptide with potential roles in mediating cardiovascular activity and is expected to become a candidate target for predicting cardiovascular diseases [6,31,32]. Increased salusin β in the brain was conducive to elevated blood pressure and sympathetic outflow in hypertensive rats [9]. However, it is not clear whether brain salusin β participates in the pathophysiological process and cardiovascular activity in hypertension-induced heart failure, and the underlying mechanisms of how salusin β affects arterial pressure, autonomic function, cardiac dysfunction and remodeling, and vascular senescence in aging SHR with heart failure require further research. Our results showed that central salusin β knockdown ameliorated cardiac and vascular function in aging SHR with heart failure dependent of reduced arterial pressure and autonomic function and that its underlying mechanisms could be attributed to the activation of ROS-relative MAPK/NF-κB pathways in the PVN.

It is well recognized that elevated blood pressure (BP), impaired autonomic function, cardiac and vascular dysfunction are the important characteristics of elderly hypertensive patients. Long-term untreated hypertension is a major cause of ventricular dysfunction and heart failure [33,34]. Recent studies also have shown that silencing salusin β using an intravenous injection of Ad-Sal-shRNA improves ventricular functions in hypertensive and diabetic cardiomyopathy rats [20,35]. Our previous study has demonstrated that central salusin β blockade attenuated elevated BP and inflammation responses in spontaneously hypertensive rats [10]. However, it is unclear whether central salusin β knockdown ameliorated peripheral manifestations of heart failure dependent of arterial pressure and autonomic function in aging SHR. Therefore, we observed the effects of central salusin β knockdown on cardiac and vascular function and analyzed the change in blood pressure and autonomic function by employing radiotelemetry in aging SHR and WKY rats. Compared with aging WKY rats, aging SHR with heart failure already manifested obvious peripheral signs, including increased left ventricular (LV) internal dimensions, decreased LVEF and LVFS, increased LVEDP and LVSP, and increased LVW/BW and LVW/Tibia ratio. Our results also indicated that vascular endothelium function was significantly impaired in aging SHR with heart failure. Interestingly, aging SHR treated with Ad-Sal-shRNA had improved cardiac and vascular function, indicating that down-regulation of salusin β in the PVN may be beneficial in attenuating the organ damage of aging SHR with heart failure. Furthermore, silencing salusin β using Ad-Sal-shRNA attenuated elevated BP and sympathetic nerve activity in aging SHR as indicated by the reduction in systolic BP and MAP, plasma norepinephrine, tyrosine hydroxylase concentrations and spectral analysis results. These results in this study suggest that the suppression of blood pressure and sympathetic activity by central salusin β knockdown may have contributed to the amelioration of cardiac and vascular function.

Increased sympathetic activity results in potentially serious ventricular arrhythmias and sudden cardiac death [36,37]. The PVN is a key integrating center for sympathetic activity and blood pressure [38,39]. Importantly, over-activity of PVN neurons has been shown to be involved in sympathetic-excitation, which participates in the pathogenesis of heart failure [19,40,41]. Interestingly, the data of this study revealed that the level of salusin β was significantly higher in the PVN of aging SHR than in aging WKY rats. More importantly, our laser confocal results demonstrated that salusin β protein is present mainly in neurons but not in the astrocytes, indicating that increased salusin β in neurons of the PVN may be an important characteristic of aged spontaneously hypertensive rats. We also found that PVN Fra-like (a marker in indicating chronic neuronal excitation) expression was greatly increased in aging SHR with heart failure. Knockdown of salusin β within the PVN resulted in reduced Fra-LI levels in aging SHR with heart failure, suggesting that brain salusin β may be a vital target for the control of chronic neuronal excitation.

An elevated central inflammatory status is a predicator of heart failure [28,39,42].Various proinflammatory cytokines (PICs) in the PVN have been associated with the severity of heart failure [39–41]. NF-κB as one of the important downstream transcription factors is responsible for the production of PICs [27,39,43]. The phosphorylation of the mitogen-activated protein kinase (MAPK) signal transduction pathway, mainly including ERK1/2, JNK1/2, and p38 MAPK subunits, is involved in the upstream regulation of NF-κB, thereby triggering the expression and activity of proinflammatory cytokines [44,45]. To confirm the mechanism by which salusin β in the PVN regulates NF-κB activation, we simultaneously observed the effect of salusin β knockdown on the MAPK signal transduction pathway. We found that the levels of PICs in the PVN were higher in the aging SHR than that in aging WKY group. Interestingly, bilateral PVN microinjections of shRNA for salusin β decreased the levels of PICs in the PVN and circulating plasma in aging SHR. Our results also showed that knockdown of salusin βsignificantly attenuated NF-κB activity and MAPK subunits in the PVN of aging SHR. These data indicate that the NF-κB and MAPK signaling pathways may be an important underlying mechanism by the knockdown of salusin β in the PVN ameliorated PVN inflammation, sympathetic excitation and heart failure.

We and others have shown that proinflammatory cytokines contribute to heart failure via induction of oxidative stress production [28,40]. Oxidative stress is characterized by increased oxidant production and impaired anti-oxidant defenses. It has been demonstrated that increased oxidative stress within the PVN of the brain plays a vital role in regulating cardiac function and maintaining sympathetic drive in SHR [41,46,47]. Therefore, we investigated whether ROS generation within the PVN of aging SHR is involved in the effects of central salusin β knockdown. The results in our study indicated that knockdown of salusin β reduces PVN oxidative stress in the aging SHR as indicated by reduced levels of NOX4, NOX2 and 4-HNE. The present study also observed that central salusin β knockdown had significantly increased T-AOC, SOD, and GSH activities, and upregulated the GSH/GSSG ratio, and decreased GSSG and MDA levels compared with that in the aging SHR treated with Ad-Scr-shRNA. Based on the above results, we deduced that silencing salusin β within the PVN attenuates cardiac and vascular function and hypothalamic inflammation possibly via ROS-relative MAPK/NF-κB pathways in the PVN of aging SHR with failure. Interestingly, the levels of superoxide in heart and mesenteric artery were also attenuated by salusin β knockdown in SHR. These results are supported by the recent study that salusin β promotes inflammatory process via the ROS/NF-κB pathway in rats with diabetic cardiomyopathy [35]. These data prompt us that superoxide is involved in the effects

of silencing salusin β in hypertension-induced heart failure. The limitations of this study are that: (i) the levels of salusin β in the heart failure patients should be measured. (ii) Further studies are needed to confirm with the ROS-relative MAPK/NF-κB pathways activators, inhibitors and their differential protein expression in aged SHR with heart failure.

5. Conclusion

In summary, our study demonstrated that central salusin β knockdown with Ad-Sal-shRNA attenuated cardiac and vascular function in aging SHR with heart failure dependent of reduced arterial pressure and autonomic function possibly via ROS-relative MAPK/NF-κB pathways in the PVN. The findings of this study provide a potential therapeutic target for hypertension-induced heart failure treatment.

Conflict of interest

All authors confirm that they are no conflicts of interest.

Acknowledgments

This study was funded by programs from National Natural Science Foundation of China (Nos. 81770426, 81700373, 81600333 and 91639105), Natural Science Foundation of Shaanxi (Nos. 2017JQ8011), China Postdoctoral Science Foundation (grant numbers 2016 M592802) and Shaanxi Postdoctoral Science Foundation (grant numbers 2016BSHEDZZ88).

Author contributions

Y. K., X. Y. and H. L. designed the study. J. B., Y. Z., Q. S., M. W., W. X. and K. L. performed all experiments. C. H., K. L., Q. Y., L. F. and W. X. also performed the data analysis and drafted the manuscript. H. L., and J. B. participated in data analysis. Y. K., H. L., X. Y., Q. S., C. H., Q. Y., J. Q. and G. Z. critically revised the manuscript. All authors reviewed the final manuscript.

Appendix A. Supplementary data

Supplementary data to this article can be found online at https://doi.org/10.1016/j.ijcard.2018.12.020.

References

[1] L.U. Pagan, R.L. Damatto, M.D. Cezar, et al., Long-term low intensity physical exercise attenuates heart failure development in aging spontaneously hypertensive rats, Cell. Physiol. Biochem. 36 (2015) 61–74.
[2] A. de la Sierra, J. Redon, J.R. Banegas, et al., Prevalence and factors associated with circadian blood pressure patterns in hypertensive patients, Hypertension 53 (2009) 466–472.
[3] D. Sueta, N. Koibuchi, Y. Hasegawa, et al., Blood pressure variability, impaired autonomic function and vascular senescence in aged spontaneously hypertensive rats are ameliorated by angiotensin blockade, Atherosclerosis 236 (2014) 101–107.
[4] U. Forstermann, T. Munzel, Endothelial nitric oxide synthase in vascular disease: from marvel to menace, Circulation 113 (2006) 1708–1714.
[5] M. Shichiri, S. Ishimaru, T. Ota, T. Nishikawa, T. Isogai, Y. Hirata, Salusins: newly identified bioactive peptides with hemodynamic and mitogenic activities, Nat. Med. 9 (2003) 1166–1172.
[6] L.L. Zhang, L. Ding, F. Zhang, et al., Salusin-beta in rostral ventrolateral medulla increases sympathetic outflow and blood pressure via superoxide anions in hypertensive rats, J. Hypertens. 32 (2014) 1059–1067 (discussion 1067).
[7] F. Takenoya, T. Hori, H. Kageyama, et al., Coexistence of salusin and vasopressin in the rat hypothalamo-hypophyseal system, Neurosci. Lett. 385 (2005) 110–113.
[8] N. Suzuki, M. Shichiri, T. Akashi, et al., Systemic distribution of salusin expression in the rat, Hypertens. Res. 30 (2007) 1255–1262.
[9] W.W. Chen, H.J. Sun, F. Zhang, et al., Salusin-beta in paraventricular nucleus increases blood pressure and sympathetic outflow via vasopressin in hypertensive rats, Cardiovasc. Res. 98 (2013) 344–351.
[10] H.B. Li, D.N. Qin, K. Cheng, et al., Central blockade of salusin beta attenuates hypertension and hypothalamic inflammation in spontaneously hypertensive rats, Sci. Rep. 5 (2015), 11162.
[11] H.J. Sun, M.X. Zhao, T.Y. Liu, et al., Salusin-beta induces foam cell formation and monocyte adhesion in human vascular smooth muscle cells via miR155/NOX2/NFkappaB pathway, Sci. Rep. 6 (2016), 23596.
[12] H.J. Sun, M.X. Zhao, X.S. Ren, et al., Salusin-beta promotes vascular smooth muscle cell migration and intimal hyperplasia after vascular injury via ROS/NFkappaB/MMP-9 pathway, Antioxid. Redox Signal. 24 (2016) 1045–1057.
[13] T. Koya, T. Miyazaki, T. Watanabe, et al., Salusin-beta accelerates inflammatory responses in vascular endothelial cells via NF-kappaB signaling in LDL receptor-deficient mice in vivo and HUVECs in vitro, Am. J. Physiol. Heart Circ. Physiol. 303 (2012) H96–105.
[14] D. Bell, E.J. Kelso, C.C. Argent, G.R. Lee, A.R. Allen, B.J. McDermott, Temporal characteristics of cardiomyocyte hypertrophy in the spontaneously hypertensive rat, Cardiovasc. Pathol. 13 (2004) 71–78.
[15] D. Graham, M.W. McBride, N.J. Brain, A.F. Dominiczak, Congenic/consomic models of hypertension, Methods Mol Med. 108 (2005) 3–15.
[16] D. Sueta, K. Kataoka, N. Koibuchi, et al., Novel mechanism for disrupted circadian blood pressure rhythm in a rat model of metabolic syndrome–the critical role of angiotensin II, J. Am. Heart Assoc. 2 (2013), e000035.
[17] H. Waki, D. Murphy, S.T. Yao, S. Kasparov, J.F. Paton, Endothelial NO synthase activity in nucleus tractus solitarii contributes to hypertension in spontaneously hypertensive rats, Hypertension 48 (2006) 644–650.
[18] J. Zubcevic, H. Waki, C. Diez-Freire, A. Gampel, M.K. Raizada, J.F. Paton, Chronic blockade of phosphatidylinositol 3-kinase in the nucleus tractus solitarii is prohypertensive in the spontaneously hypertensive rat, Hypertension 53 (2009) 97–103.
[19] G.S. Masson, A.R. Nair, P.P. Silva Soares, L.C. Michelini, J. Francis, Aerobic training normalizes autonomic dysfunction, HMGB1 content, microglia activation and inflammation in hypothalamic paraventricular nucleus of SHR, Am. J. Physiol. Heart Circ. Physiol. 309 (2015) H1115–H1122.
[20] X.S. Ren, L. Ling, B. Zhou, et al., Silencing salusin-beta attenuates cardiovascular remodeling and hypertension in spontaneously hypertensive rats, Sci. Rep. 7 (2017), 43259. .
[21] H.B. Li, D.N. Qin, L. Ma, et al., Chronic infusion of lisinopril into hypothalamic paraventricular nucleus modulates cytokines and attenuates oxidative stress in rostral ventrolateral medulla in hypertension, Toxicol. Appl. Pharmacol. 279 (2014) 141–149.
[22] Y. Yu, S.G. Wei, Z.H. Zhang, R.M. Weiss, R.B. Felder, ERK1/2 MAPK signaling in hypothalamic paraventricular nucleus contributes to sympathetic excitation in rats with heart failure after myocardial infarction, Am. J. Physiol. Heart Circ. Physiol. 310 (2016) H732–H739.
[23] B. Kisso, A. Patel, R. Redetzke, A.M. Gerdes, Effect of low thyroid function on cardiac structure and function in spontaneously hypertensive heart failure rats, J. Card. Fail. 14 (2008) 167–171.
[24] R.K. Sharma, A.C. Oliveira, S. Kim, et al., Involvement of neuroinflammation in the pathogenesis of monocrotaline-induced pulmonary hypertension, Hypertension 71 (2018) 1156–1163.
[25] L. Cao, Y.X. Cao, C.B. Xu, L. Edvinsson, Altered endothelin receptor expression and affinity in spontaneously hypertensive rat cerebral and coronary arteries, PLoS One 8 (2013), e73761.
[26] R.B. Dange, D. Agarwal, R. Teruyama, J. Francis, Toll-like receptor 4 inhibition within the paraventricular nucleus attenuates blood pressure and inflammatory response in a genetic model of hypertension, J. Neuroinflammation 12 (2015) 31.
[27] H.B. Li, X. Li, C.J. Huo, et al., TLR4/MyD88/NF-kappaB signaling and PPAR-gamma within the paraventricular nucleus are involved in the effects of telmisartan in hypertension, Toxicol. Appl. Pharmacol. 305 (2016) 93–102.
[28] Y.M. Kang, Y. Ma, C. Elks, J.P. Zheng, Z.M. Yang, J. Francis, Cross-talk between cytokines and renin-angiotensin in hypothalamic paraventricular nucleus in heart failure: role of nuclear factor-kappaB, Cardiovasc. Res. 79 (2008) 671–678.
[29] Y.K. Wang, Q. Yu, X. Tan, et al., Centrally acting drug moxonidine decreases reactive oxygen species via inactivation of the phosphoinositide-3 kinase signaling in the rostral ventrolateral medulla in hypertensive rats, J. Hypertens. 34 (2016) 993–1004.
[30] Q. Su, J.J. Liu, W. Cui, et al., Alpha lipoic acid supplementation attenuates reactive oxygen species in hypothalamic paraventricular nucleus and sympathoexcitation in high salt-induced hypertension, Toxicol. Lett. 241 (2016) 152–158.
[31] K. Sato, R. Watanabe, F. Itoh, M. Shichiri, T. Watanabe, Salusins: potential use as a biomarker for atherosclerotic cardiovascular diseases, Int. J. Hypertens. 2013 (2013) 965140.
[32] M. Nagashima, T. Watanabe, Y. Shiraishi, et al., Chronic infusion of salusin-alpha and -beta exerts opposite effects on atherosclerotic lesion development in apolipoprotein E-deficient mice, Atherosclerosis 212 (2010) 70–77.
[33] M.H. Drazner, The progression of hypertensive heart disease, Circulation 123 (2011) 327–334.
[34] A. Diwan, G.W. Dorn 2nd, Decompensation of cardiac hypertrophy: cellular mechanisms and novel therapeutic targets, Physiology (Bethesda) 22 (2007) 56–64.
[35] M.X. Zhao, B. Zhou, L. Ling, et al., Salusin-beta contributes to oxidative stress and inflammation in diabetic cardiomyopathy, Cell Death Dis. 8 (2017) e2690.
[36] S.G. Wei, Y. Yu, R.M. Weiss, R.B. Felder, Endoplasmic reticulum stress increases brain MAPK signaling, inflammation and renin-angiotensin system activity and sympathetic nerve activity in heart failure, Am. J. Physiol. Heart Circ. Physiol. 311 (2016) H871–H880.
[37] S.G. Wei, Y. Yu, R.M. Weiss, R.B. Felder, Inhibition of Brain mitogen-activated protein kinase signaling reduces central endoplasmic reticulum stress and inflammation and sympathetic nerve activity in heart failure rats, Hypertension 67 (2016) 229–236.
[38] O.M. Ogundele, C.C. Lee, J. Francis, Age-dependent alterations to paraventricular nucleus insulin-like growth factor 1 receptor as a possible link between sympathoexcitation and inflammation, J. Neurochem. 139 (2016) 706–721.

[39] Y.M. Kang, F. Gao, H.H. Li, et al., NF-kappaB in the paraventricular nucleus modulates neurotransmitters and contributes to sympathoexcitation in heart failure, Basic Res. Cardiol. 106 (2011) 1087–1097.
[40] A. Guggilam, M. Haque, E.K. Kerut, et al., TNF-alpha blockade decreases oxidative stress in the paraventricular nucleus and attenuates sympathoexcitation in heart failure rats, Am. J. Physiol. Heart Circ. Physiol. 293 (2007) H599–H609.
[41] A. Guggilam, J.P. Cardinale, N. Mariappan, S. Sriramula, M. Haque, J. Francis, Central TNF inhibition results in attenuated neurohumoral excitation in heart failure: a role for superoxide and nitric oxide, Basic Res. Cardiol. 106 (2011) 273–286.
[42] Y.M. Kang, Z.H. Zhang, R.F. Johnson, et al., Novel effect of mineralocorticoid receptor antagonism to reduce proinflammatory cytokines and hypothalamic activation in rats with ischemia-induced heart failure, Circ. Res. 99 (2006) 758–766.
[43] M. Rahimifard, F. Maqbool, S. Moeini-Nodeh, et al., Targeting the TLR4 signaling pathway by polyphenols: a novel therapeutic strategy for neuroinflammation, Ageing Res. Rev. 36 (2017) 11–19.
[44] Y.H. Son, Y.T. Jeong, K.A. Lee, et al., Roles of MAPK and NF-kappaB in interleukin-6 induction by lipopolysaccharide in vascular smooth muscle cells, J. Cardiovasc. Pharmacol. 51 (2008) 71–77.
[45] J. Ghosh, J. Das, P. Manna, P.C. Sil, Taurine prevents arsenic-induced cardiac oxidative stress and apoptotic damage: role of NF-kappa B, p38 and JNK MAPK pathway, Toxicol. Appl. Pharmacol. 240 (2009) 73–87.
[46] Y.M. Kang, Z.H. Zhang, B. Xue, R.M. Weiss, R.B. Felder, Inhibition of brain proinflammatory cytokine synthesis reduces hypothalamic excitation in rats with ischemia-induced heart failure, Am. J. Physiol. Heart Circ. Physiol. 295 (2008) H227–H236.
[47] X.J. Yu, Y.P. Suo, J. Qi, et al., Interaction between AT1 receptor and NF-kappaB in hypothalamic paraventricular nucleus contributes to oxidative stress and sympathoexcitation by modulating neurotransmitters in heart failure, Cardiovasc. Toxicol. 13 (2013) 381–390.